Pharmacogn. Mag.
A multifaceted peer reviewed journal in the field of Pharmacognosy and Natural Products
www.phcog.com | www.phcog.net

ORIGINAL ARTICLE

Fracture Healing in SD Rats' Bioactivities of Cucumber Seed Polysaccharides

Zhihong Zhang[1], Yuanning Zeng[2], Donghui Peng[1], Na Xing[3], Haodong Bai[1], Yuxin Li[1], Na Cui[1], Huilin Su[2], Tingting Qiao[2], Congjing Shi[2], Haixue Kuang[1], Qiuhong Wang[1,2]

[1]Department of Chinese Medicine Processing, Key Laboratory of Chinese Materia Medica, Heilongjiang University of Chinese Medicine, Ministry of Education, Harbin, [2]Department of Chinese Medicine Processing, School of Traditional Chinese Medicine, Guangdong Pharmaceutical University, Guangzhou, [3]Zhongshan Institute for Drug Discovery, Zhongke Zhongshan Institute of Drug Innovation, Zhongshan, China

Submitted: 12-Jan-2022 Revised: 21-May-2022 Accepted: 19-Jul-2022 Published: 19-Sep-2022

ABSTRACT

Aim/Background: We investigated the composition and structure of intracellular polysaccharides in cucumber seeds (CSs) and their effect on Sprague-Dawley (SD) rats and potential activity for fracture healing. **Materials and Methods:** Polysaccharides are its main water-soluble active ingredient. The SD rat tibia fracture model was established by surgical method, and the healing effect of cucumber seed polysaccharides (CSPs) on SD rat tibia fracture was preliminarily explored. Through histopathological observation, determination of rat serum indicators alkaline phosphatase (AKP), acid phosphatase (ACP), BGP, X-ray imaging observation, and micro-Computed Tomography (CT) imaging observation at different periods. **Results and Conclusion:** The results showed that CSP enhanced the activity of osteoblasts, increased the metabolic rate of osteoclasts, increased the secretion of AKP, BGP, and ACP, shortened the fracture healing time of SD rats and effectively promoted the healing of tibial fractures in SD rats.

Key words: Cucumber seeds, extraction of polysaccharides, fracture healing, polysaccharides, SD rats

SUMMARY

- The results showed that CSP enhanced.
- CSP has a great potential in promoting fracture healing in SD rats.The activity of osteoblasts, increased the metabolic rate of osteoclasts,increased the secretion of AKP, BGP, and ACP, shortened the fracture healing time of SD rats and effectively promoted the healing of tibial fractures in SD rats.

Abbreviations used: CS: Cucumber seed; CSP: Cucumber seeds polysaccharide; DDP: Dieda Pill; AKP: Alkaline phosphatase; ACP: Acid phosphatase; BGP: Osteocalcin; BV: Bone volume; TV: Total volume.

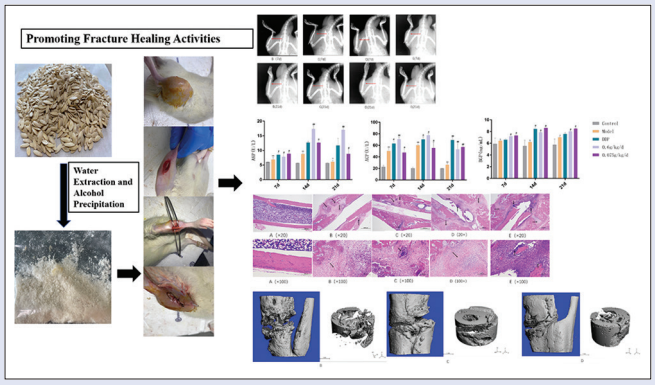

Correspondence:
Prof. Haixue Kuang,
Key Laboratory of Chinese Materia Medica,
Heilongjiang University of Chinese Medicine,
Ministry of Education, Harbin - 150040, China.
E-mail: hxkuang@hljucm.net
Prof. Qiuhong Wang,
Key Laboratory of Chinese Materia Medica,
Heilongjiang University of Chinese Medicine,
Ministry of Education, Harbin - 150040, China.
E-mail: qhwang668@sina.com
DOI: 10.4103/pm.pm_14_22

Access this article online
Website: www.phcog.com
Quick Response Code:

INTRODUCTION

A fracture is a complete or partial break in the continuity of the bone structure. It is more common in children and the elderly, and it also occurs in young and middle-aged people.[1] With the increase in global ageing, the incidence of fractures is on the rise with the increase of fractures. Fracture healing is a complex physiological process with the formation of local hematoma and local inflammation.[2] The healing process involves the proliferation, differentiation and matrix mineralization of osteoblasts. Traditional Chinese Medicine (TCM) promotes fracture healing by controlling inflammation, promoting blood circulation, and stimulating bone regeneration.[3] Some TCMs have shown therapeutic effects on fracture healing in clinical and animal studies, to some extent, it is reasonable to assume that some TCMs influence the process of bone metabolism and bone formation.[4] Cucumber seed (CS) mainly contain sugars and glycosides, triterpenes, phytosterols, fatty acids, amino acids, and other components.[5,6] Furthermore, CSs are often used for fractures, tendon injuries, rheumatic arthralgia, fatigue and cough, and CS is the dried riped seeds of *Cucumis satiuus* L., a medicinal and food homologous plant of the Cucumber family, also known as Halisu. In summer and autumn, CS was obtained by drying. It is sweet in taste, flat in nature, and belongs to the liver and lung meridians. The chemical components in CS mainly contained polysaccharides, glycosides, amino acids, phytosterols, triterpenes, fatty acids, and other chemical components.[7] There are many studies on the small molecular components in CS, however, there is almost no research on its macromolecular polysaccharides. Furthermore, in this paper extracted cucumber seed polysaccharide (CSP) from CS, and preliminarily studied the effect of CSP in promoting fracture healing in SD rats. Further deepen the understanding of the pharmacological effects of the traditional Chinese medicine CSP, to provide a reference

Cite this article as: Zhang Z, Zeng Y, Peng D, Xing N, Bai H, Li Y, *et al*. Fracture healing in SD rats' bioactivities of cucumber seed polysaccharides. Phcog Mag 2022;18:738-45.

for the rational development and utilization of the active polysaccharide in CS.

MATERIALS AND METHODS

Plant materials and reagents

Dried CS was purchased from the Hebei Anguo Medicinal Materials Market in 2019 and was identified by professor Jizhu Liu of Guangdong Pharmaceutical University (GDPU). The samples were packed and stored in an airtight container at room temperature. The alkaline phosphatase (AKP) kit (20201012) and acid phosphatase (ACP) kit (202001012) was purchased from Nanjing Jiancheng Biological Engineering Research Institute (China). Osteocalcin (BGP) kit (2020081113) was purchased from Jiangsu Meimian Biological Engineering Research Institute (China), D-Mannose (Man), L-rhamnose (Rha), D-glucose (Glc), D-galactose (Gal), D-xylose (Xyl), L-fucose (Fuc) were obtained from Sigma-Aldrich (St. Louis, MO, USA). Unless otherwise stated, all of the other reagents were of analytical grade.

Extraction from CS

The extraction of polysaccharide was described below. Briefly, CS was defatted by ethanol (80%, v/v) at 100°C three times (2 hr each time) and then extracted by 700 mL of water at 100°C three times (2 hr each time). The extracts were concentrated and cooled at room temperature.[8] Then 85% ethanol was added to extracts until the final concentration reached 75% (v/v) for the precipitates. After being incubated at 4°C three times (48 hr each time), the precipitates were obtained by centrifugation (4000 rpm for 15 min).[9] The precipitates were washed three times (30 min each time) alternately with absolute ethanol and acetone. After that, the dialysis liquid was collected and lyophilized to obtain CSP.

Molecular weight determination

The molecular weight of CSP was detected by the High Performance Liquid Chromatography (HPLC)- Evaporative light Scattering Detector (ELSD). A series of dextran standards (Mw: 10,40,70,500 and 2000 kDa) with concentration 2 mg/mL were utilized to draw the exclusion curve. The chromatographic conditions were based on the other research and the liquid flow rate was 0.7 mL/min.[10] A standard curve with the lg value (x) of the molecular weight of each standard as the abscissa was a draw and the retention time (y) as the abscissa. In addition, the CSP was dissolved in water to prepare a sample solution with a mass concentration of 2 mg/mL for measurement. Ultimately, the aqueous layer was filtered through a 0.45 μm membrane and analyzed by HPLC.[11]

Monosaccharide composition analysis

The monosaccharide composition of CSP was detected by high-performance liquid chromatography via the precolumn derivatization of 1-phenyl-3-methyl-5-pyrazolone (PMP).[12]

After 15 mg of polysaccharide sample was placed in a 10 ml stoppered test tube, the 2 ml of 2 mol/L TFA solution was added into the tube, which was hydrolysis at 120°C for 160 min. The hydrolysate solution was obtained finally.[13] The remaining TFA was removed by distillation under reduced pressure. During the period, methanol was added, and the distillation was repeated 3-4 times until there was no sour taste, and double-distilled water was added to dilute to 2 ml.

After taking 1 mg standard monosaccharide reference substance and 2 ml mixed monosaccharide reference substance, they were placed in 5 ml centrifuge tubes, respectively. After 400 μl of the above solution was taken out, 200 μl 0.5 mol/L PMP methanol solution and 200 μl 0.3 mol/L NaOH solution were added into each centrifuge tube in turn. The mixed samples were placed in a 70°C water bath for heating and reaction for 30 min.[14] Then 200 μl 0.3 mol/L HCl solution was added to the solution to neutralize. After that, equal volumes of isoamyl acetate and chloroform were added successively to extract four times. Ultimately, the aqueous layer was filtered through a 0.45 μm membrane and analyzed by HPLC.[15]

The chromatography was conducted using Waters Acquity Arc (USA) equipped with a SunFire C18 (5 μm, 4.6 × 250 mm) and a 2489 UV detection wavelength of 254 nm. The mobile phase was a acetonitrile (20% ~23% ~24% ~30%) and 0.1% formic acid water, the flow rate was 1 mL/min, and the sample injection volume was 10 μL.[16]

Treatment of fracture healing using CSP

Animals

Forty male SD rats (180 ± 200 g) were purchased from Guangdong Medical Laboratory Animal Center (SCXK2018-0002). Animals were kept under a 12 hr light-dark cycle at 24 ± 2°C, with 50% ± 5% relative humidity and were freely given access to water and standard chow. The experiments were carried out according to the rules for use of the laboratory animals issued by the GDPU and protocols were approved by the Animal Ethics Committee of GDPU.

Model establishment and treatment

The SD rats were adapted to the environment for one week and then modeled. The rats were fasted and watered 12 hr before modeling. The SD rats were given an intraperitoneal injection of pentobarbital sodium (50 mg/kg, 3 mg/ml) for anesthesia, and penicillin was injected intramuscularly into SD rats in the operation group at 50 g/kg. After the anesthesia takes effect, the rat was placed in the right prone position and fix it. The hair of the rat's left leg tibia was removed by depilatory cream. The skin of the depilated area was disinfected by using iodophor [Figure 1a]. A 1.5 cm long longitudinal incision in the skin was scratched [Figure 1b], and the muscles around the tibia of the rat were bluntly separated by using tweezers to expose the tibia clearly and then using two curved tweezers to support the fully exposed tibia [Figure 1c]. Ultimately, the tibia was cut completely with an orthopedic vision. An appropriate length of Kirschner with 1 mm diameter was inserted from the fractured end to the proximal end of the tibial diaphysis into the medullary cavity; passing the tip of the Kirschner wire from the greater trochanter of the tibia. The two ends of the fracture were reduced and the Kirschner wire was threaded back from the bone marrow cavity after reduction. Before suturing the muscle and epidermal surgical site, the surgical bone was moved.[17] After confirming that the site to be operated is firmly fixed, the excess part of the Kirschner wire was bending and cut it off. Rinsing with normal saline, before suturing layer by layer [Figure 1d], and give an intramuscular injection of gentamicin sulfate to the surgical site for three consecutive days for anti-inflammatory and to prevent infection.

The random number method was used to group 40 SPF male SD rats after adaptive feeding for 1 week. Group a was treated as a sham operation group (no model was made and normal saline was given). Group b is the model group (modeling and administration of saline). Group c is the Dieda Pill group, administered at 0.6 g/kg/day(s), as the positive control group. The d1 group is the CSP high-dose group, and the administration does is 0.6 g/kg/day(s). Group d2 is the CSP low-dose group, and the dosage is 0.075 g/kg/day(s). CSP and Dieda Pills were converted into a rat's drug dosage according to the clinical dosage of an adult (based on a bodyweight of 60 kg). Dieda Pills and CSP powder were prepared into suspensions with distilled water. The rats in the administration group were given gastric administration on the second day after the model was established, and the rats were given intragastric administration

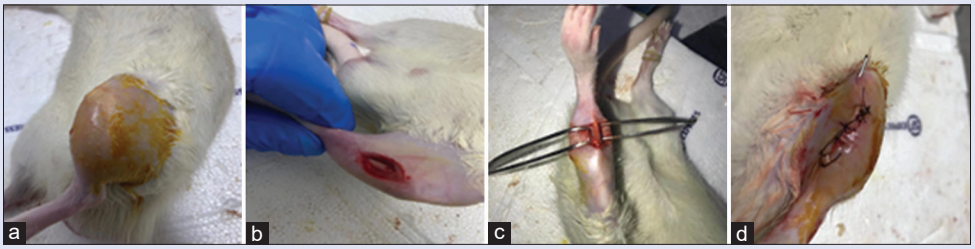

Figure 1: a: Perform skin preparation; b: Cut the skin; c: Fully expose the femur; d: Insert the Kirschner wire, reset the broken end of the fracture, and perform suture

once a day at 9 o'clock in the morning for 28 consecutive days to obtain materials. The blank control group and the model control group were given normal saline, and blood was taken from the orbit on the 7, 14, and 21 days after administration for serum index determination.

X-ray examinations

After 7 and 21 days of the first postoperative administration, 3 mice in each of the CSP high-dose, low-dose group, model group, and Dieda pill group were taken for routine orthotopic rat tibia X-ray imaging. X-rays of the left hind limb were taken under pentobarbital sodium anesthesia, with 5000 V parameters and 6.0 sec exposure time. Observe the location, type, and shape of the fracture line.[18]

Histopathological observation

After putting the paraffin sections in xylene I for 20 min, they were taken out and put in xylene II for 20 min. Then they were taken out and put in anhydrous ethanol I for 5 min, putting them in anhydrous ethanol II for 5 min, then taking them out and putting them in 75% alcohol for 5 min, and finally washing them with tap water. The slices firstly were put after the above treatment into hematoxylin staining solution for 3-5 min. After washing with tap water, the differentiation solution was taken for differentiation treatment, rinsing with tap water, adding the blue-back solution, and rinsing with running water. To take the slices and put them in 85% ethanol for dehydration for 5 min, and then put the slices in 95% ethanol for dehydration for 5 min. Staining in eosin staining solution for 5 min, absolute ethanol I was first added to the slices and soaked for 5 min, then soaked the slices in absolute ethanol II for 5 min, and finally, absolute ethanol III was added to soak for 5 min. Xylene I was used for transparent treatment for 5 min, and then xylene II was added to the transparent treatment for 5 min. The above-mentioned processed slices are mounted with neutral gum. Finally, using a microscope for microscopic examination and image acquisition and analysis.[18]

Determination of AKP and ACP levels in serum by micro-enzyme assay

At 7, 14, and 21 days after the first administration, the blood was taken from the orbit of the rat *in vivo*, centrifuged to take the supernatant, and stored at -20°C for the determination of AKP and ACP levels. The specific operation steps are as follows. Take out 5 μL serum sample and add 50 μL of buffer and matrix solution to mix thoroughly. When adding samples, the speed and strength of the sample should be noted and adding sample to the bottom to avoid an incomplete reaction. The plate was placed in an air bath at 37°C for 15 min and then 150 μL of chromogenic reagent was added. Gently shake the plate to mix well. The absorbance OD value of each well was measured by a microplate reader at a wavelength of 520 nm, and finally, the AKP content in the serum of fractured rats was calculated. The 4 μL of the serum sample was mixed with 40 μL of buffer and 40 μL of matrix solution to react. The above-mentioned orifice plate was put in a 37°C air bath for 30 min and then added 80 μL of lye and 80 μL of the color developer to each hole, and gently shaking it. After standing for 10 min, the OD value of each well was measured by a microplate reader at a wavelength of 520 nm, and finally, the ACP content in the serum of the fractured rat was calculated.[19]

Enzyme-linked immunoassay to determine the level of BGP in serum

At 7, 14, and 21 days after the first administration, the blood was taken from the *in vivo* orbit of the rats, centrifuging and taking the supernatant, and stored at -20°C to determine the level of BGP in the serum. The specific operation steps are as follows. Blank wells, standard wells, and sample wells are to be tested on the enzyme-labeled coated plate. Firstly, 50 μL of the standard substance was added to the enzyme-labeled coating plate, then adding 40 μL of the sample diluent to the test sample well, and then adding 10 μL of the test sample to it. After adding the sample, gently shake and mix at the bottom of the well of the microtiter plate, and take care not to touch the wall of the well as much as possible. The plate was placed with a sealing film at 37°C for 30 min. Use distilled water to dilute the 30-fold concentrated washing solution 30-fold before using. After tearing off the sealing film, the liquid was discarded in each well and spun dry, and fill each well with washing liquid. Let it stand for 30 sec and then discard, repeat 5 times and pat dry. The 50 μL of enzyme-labeled reagent was added to each well except the blank well. The plate was sealed again with the sealing film and incubated at 37°C for 30 min. After tearing off the sealing film, the liquid was discarded and spun dry. The washing solution was filled in each well, then it was discarded after it stood for 30 sec. After adding 50 μL of developer A to each well, 50 μL of developer B was added to it. After gently shaking and mixing, the well plate was developed in the dark for 10 min at 37°C. The 50 μL of stop solution was added to each well to terminate the reaction. After the reaction was terminated, the blue turns yellow. The blank holes were used for zero adjustments, and the absorbance (OD value) of each hole was measured at a wavelength of 450 nm. The measurement was completed within 15 min after adding the stop solution.

Micro-CT examinations

(1) The sample was taken out of the paraformaldehyde fixing solution and wrapped with plastic film to keep moisture. It was put into a 19 mm diameter sample tube, putting cotton around the bone tissue to fix it. The sample perpendicular was saved to the sample tube when fixed and then put into the scanning instrument (SCANCO MEDICALμCT100) for scanning. (2) Perform Micro-CT (SCANCO MEDICALμCT100) detection on the sample. When scanning, the X-ray beam scans perpendicular to the surface of the sample. The scanning parameters selected by μCT100 are: scanning energy intensity: 70 KVp, 200 μA, 8 W; filter: 0.5 AL; CT value is corrected at 1200 mgHA/cm; image matrix: 8192X 8192; FOV (field of view) 20.48 mm, resolution 10 μm,

Sampletim (exposure time) 300 ms; (3) After the scan was completed, the Micro-CT system will automatically reconstruct the sample in two dimensions, open the SCANCOμCT Evaluation Promgram V6.6 software to perform data analysis and three-dimensional reconstruction of the sample: According to bone fracture Position, draw a circle with a diameter of 5 mm as the Region of Interest (ROI), and select 8 mm as the fracture position. Set the bone threshold to 120-1000; after the threshold is set, perform data analysis and three-dimensional reconstruction. After the 3D image comes out, open the μCT Ray V4.2 software to rotate to a uniform angle, and export the 3D image after loading.[20,21]

Statistical analysis

The experimental data were compared between groups and calculated by GraphPad Prism 7.0 software. One-way analysis of variance is obtained by comparison between groups, and $P < 0.05$ indicates that the data is significantly different. The number of samples in each group of experiments is ≥3, and the experimental data results in each group are expressed as mean ± variance ($\bar{X}$ ± SD), and are calculated by Microsoft Excel 2019 software.[22]

RESULTS

Molecular weight determination

HPLC was used to detect the polysaccharide molecular weight. It is widely recognized as the most authoritative test to date. Figure 2 shows the standard curve plotted from the molecular weights and retention times of five dextran. The molecular weight range of CSP obtained by substituting the retention time of CSP into the standard curve of dextran is $1.1 \times 10^7 \sim 2.53 \times 10^7$ kDa.

Monosaccharide composition analysis

The monosaccharide composition analysis of the PMP pre-column HPLC results indicated that CSP was composed of mannose, ribose, rhamnose, galactose, glucose, arabinose, glucuronic acid, and galacturonic acid in Figure 3. The results further suggested that CSP was a heteropolysaccharide. Furthermore, the results showed that galactose, arabinose, glucuronic acid, and galacturonic acid were the most abundant monosaccharides.

X-ray examinations observation

After seven days of administration, the SD rats in each treatment group had obvious clearances at the tibial fractures, indicating that no ossified callus was formed. In Figure 4b, after 21 days of the administration, there was a wide transparent area between the fracture ends of the SD rats in the model group, and the hematoma at the operation site was not completely absorbed. In Figure 4d, CSP high-dose group produced callus outside the cells, and the hematoma was basically absorbed and replaced by granulation tissue. When the bone-like tissue and trabecular bone appear, the fracture ends become blurred, the amount of callus increases and deepens, and the gap between fractures is not obvious. In Figure 4e, the CSP low-dose group was absorbed, and the gap between the fractures was more obvious. After 21 days of the administration, the fracture ends of SD rats in the Dieda Pill group in Figure 4c (21d) were blurred, and the bone density increased significantly. The degree of fracture healing in the high-dose CSP group Figure 4d was similar to that in the Dieda Pill group.

Histopathological observation

Figure 5a (×20) and (×100) are bone tissues that have not been modeled. The Figure shows that there is no obvious fracture or damage in the tissue, the thickness of the bone cortex is uniform, and there is no obvious bone hyperplasia; hematopoiesis in the marrow cavity is rich in cells. Figure 5b (×20) and (×100) are the model group. From the figures, it can be seen that most of the bone marrow disappears, and connective tissue hyperplasia and some necrotic materials can be seen; at the same time, the local injury is uplifted, and a small amount of hyperplasia of bone and a large amount of semicolon can be seen. There is no connection on one side, and some necrosis is visible. Figure 5c (×20) and (×100)are the positive drug group. It can be seen from the Figure that most of the bone marrow disappears, and connective tissue hyperplasia can be seen; proliferation of cartilage cells can be seen at the joint of the bone on one side of the injury. The connective tissue and some bone fragments, and individual pyogenic necrosis can be seen. Figure 5d (×20) and (×100) are CSPs in high-dose groups. From Figure 5, some residual bone fragments, connective tissue hyperplasia, and a large number of neutrophil infiltration; two injuries of the side bones are connected by connective tissue and cartilage, which can be seen that most of the bone marrow disappears. Figure 5e (×20) and (×100) are CSPs in low-dose groups. From the Figure, it can be seen that most of the bone marrow disappears, and there are more residual bone fragments, connective

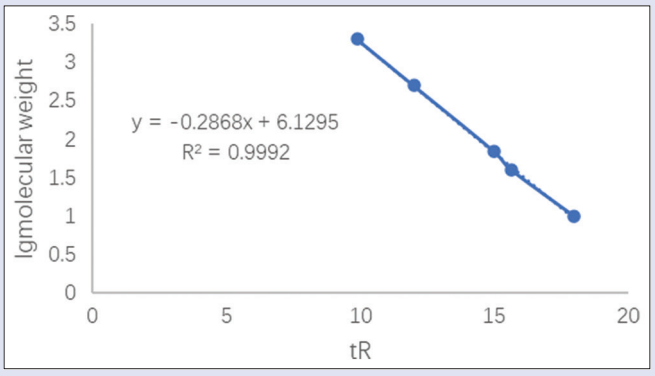

Figure 2: Dextran standard curve chart

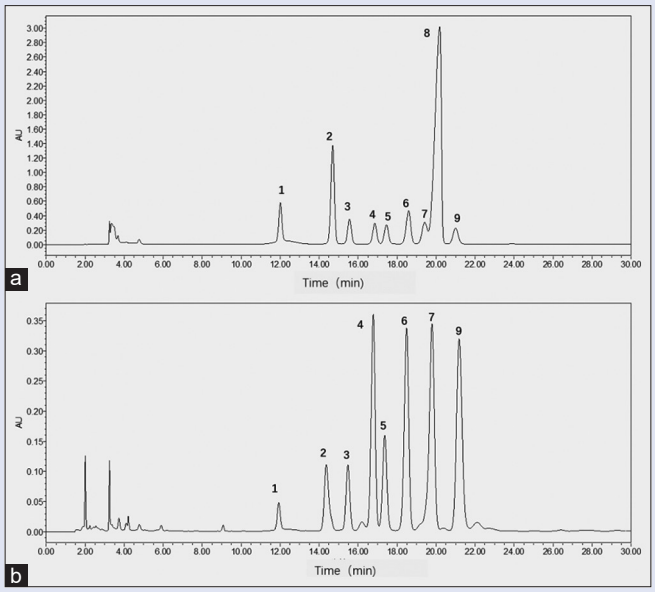

Figure 3: HPLC analysis of PMP pre-column derivatives of (a) nine standard monosaccharides. (1. mannose; 2. Ribose; 3. rhamnose; 4. galactose; 5. glucose; 6. arabinose; 7. glucuronic acid; 8. xylose; 9. galacturonic acid) and (b) CSP hydrolysate

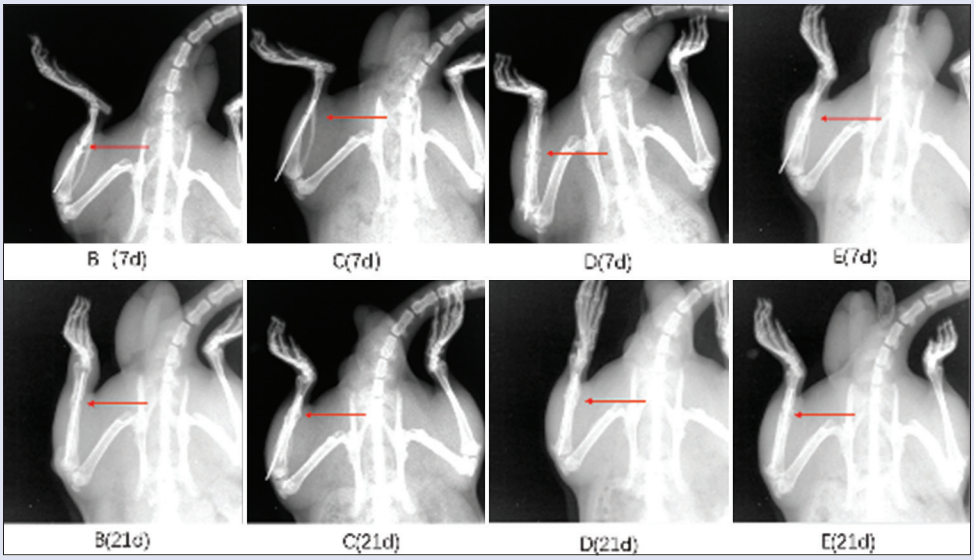

Figure 4: Tibia X-rays of rats at 7 days and 21 after operation (B: model group; C: positive drug group; D: cucumber seed polysaccharides high-dose group; E: cucumber seed polysaccharides low-dose group)

tissue hyperplasia, and a large number of neutrophil infiltration. The side bones are connected by cartilage tissue.

Detection of the ALP, ACP, and BGP in serum

It can be seen from Figure 6 that after seven days of the administration that the serum AKP level of the model group was higher than that of the blank control group ($P < 0.05$), and the positive control group and the polysaccharide high- and low-dose groups were higher than the model group ($P < 0.05$). After 14 days of the administration, the serum AKP levels of the rats in the positive control group and the high- and low-polysaccharide dose groups were significantly higher than those in the model group ($P < 0.01$). After 21 days of the administration, the fracture sites of the rats in each operation group began to heal. The serum AKP levels of the rats in the positive control group and the high- and low-dose polysaccharide groups began to decline, but they were still significantly higher than the model group ($P < 0.05$).

It can be seen from Figure 7 that after seven days of administration, the serum ACP level of rats in the model group was significantly higher than that of the blank control group ($P < 0.01$), and the serum ACP level of rats in the positive drug group and the high and low doses of polysaccharides was higher than that of the model group ($P < 0.05$). After 14 days of administration, the serum level of rats in the model group was similar to that of the positive drug group, but the model group is lower than that of the polysaccharides high-dose group. This may be because the osteoclasts of the model group absorbed necrotic bone and cleared the residue faster than the low-dose polysaccharide group. After 21 days of administration, the serum ACP levels of rats in the positive drug group and polysaccharides high- and low-dose groups were significantly higher than those in the model group ($P < 0.01$).

It can be seen from Figure 8 that after seven days of administration, the serum BGP level of rats in the model group was higher than that of the blank control group, and the serum BGP level of rats in the positive drug group and the high- and low-dose polysaccharides groups was higher than that in the model group but not significant. After 14 days of administration, the serum BGP levels of rats in the positive drug group and the high- and low-dose polysaccharide groups were significantly higher than those in the model group ($P < 0.05$). After 21 days of administration, the serum BGP level of the rats in the positive drug group and the high- and low-dose polysaccharides groups was higher than that in the model group, but it is not significant. This may be because the fracture site of the rat at this time has healed and the specific secretion of osteoblasts and is caused by the gradual decline in the activity of the protein.

Micro-CT examinations observation

BV represents bone volume, which refers to the trabecular bone part. TV represents tissue volume, which refers to the trabecular bone part and the hollow part (excluding the bone part). It can be seen from Figure 9a,b that the sagittal and coronal cross-sectional views of the model group. The positive drug group and the polysaccharides high-dose group are selected. After 28 days of the administration, the callus at the fractured end of the rats in the high-dose polysaccharide group and the positive drug group were increased, and the fracture line of the fractured end was not obvious, however, the callus shaped fracture was close to the healing. Three-dimensional reconstruction of the callus at the fractured end of the middle tibia in the polysaccharide high-dose group Figure 9d and the positive drug group Figure 9c, the bone density and trabecular shape of the two groups became thicker. Compared with the model group Figure 9b, the callus plate-shaped trabecula was half in the polysaccharides-administered group Figure 9d and in the positive drug group Figure 9c, the trabecula was regular plate-shaped, and the fracture line disappeared. According to Table 1, compared with the model group, the bone volume/tissue volume (BV/TV) ratio of the polysaccharide high-dose group and the positive drug group were significantly increased, with significant differences ($P < 0.05$). It shows that CS polysaccharides can effectively promote the increase of callus volume and the number of osteoblasts, and effectively promote the formation of callus. Therefore, the healing of rat fractures was promoted.

After the mechanical integrity of bone is lost, fractures will occur, and local soft tissues and blood vessels will also be damaged.[23] Fracture healing is an extremely complex process. There are a variety of tissues and cells involved, mainly including osteoblasts and osteoclasts.[24] The activity of osteoblasts can be reflected by detecting the content of serum BGP and osteoclasts. The activity of ACP can be reflected by detecting the level of ACP in the serum. Fracture healing is mainly completed

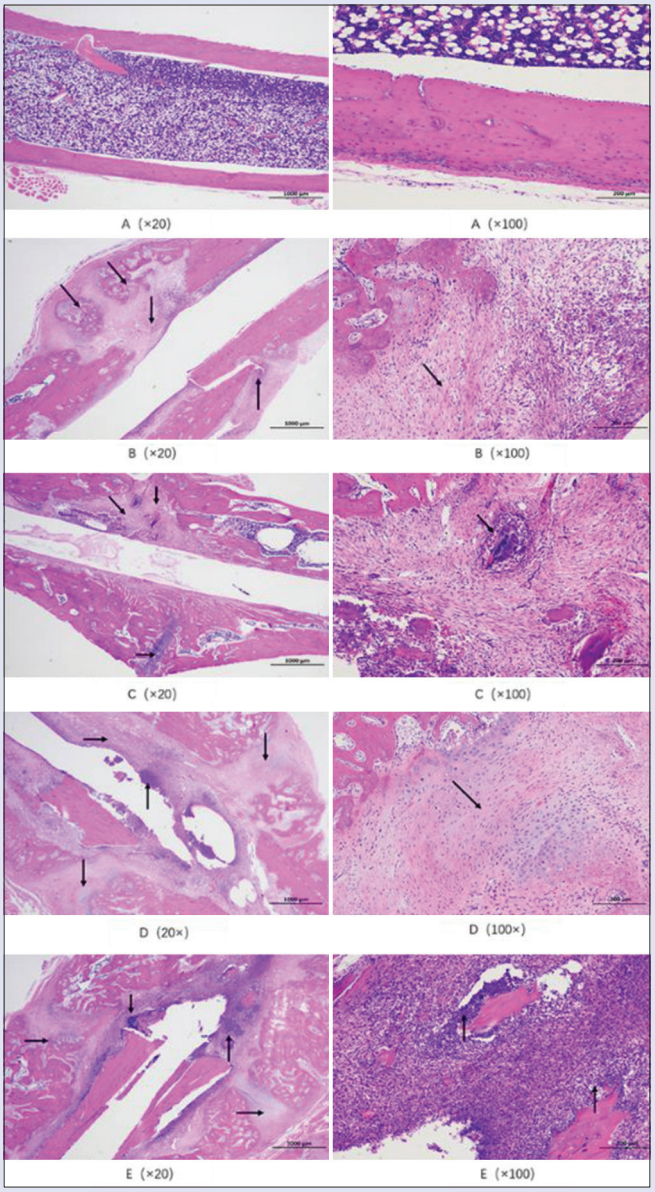

Figure 5: Pathological section of rat tibia A: Blank group; B: Model group; C: Positive drug group; D: Cucumber seed polysaccharides high-dose group; E: Cucumber seed polysaccharides low-dose group

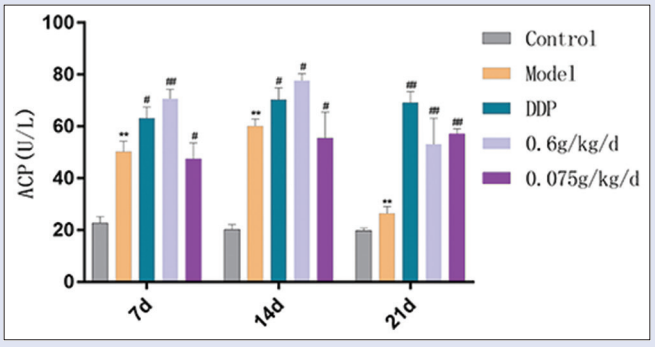

Figure 7: ACP changes in rats in different experimental groups ($\bar{X}$ ± SD, n = 8) (Compared with the blank group, $P < 0.01$ is **, $P < 0.05$*; compared with the model group, $P < 0.01$ is $^{\#\#}$, $P < 0.05$ is $^{\#}$)

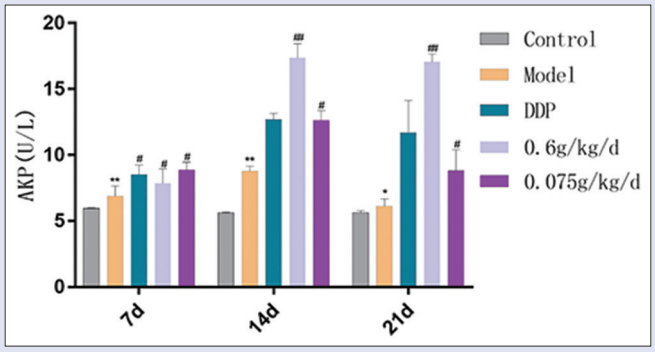

Figure 6: The AKP changes of rats in different experimental groups ($\bar{X}$ ± SD, n = 8) (Compared with the blank group, $P < 0.01$ is **, $P < 0.05$*; compared with the model group, $P < 0.01$ is $^{\#\#}$, $P < 0.05$ is $^{\#}$)

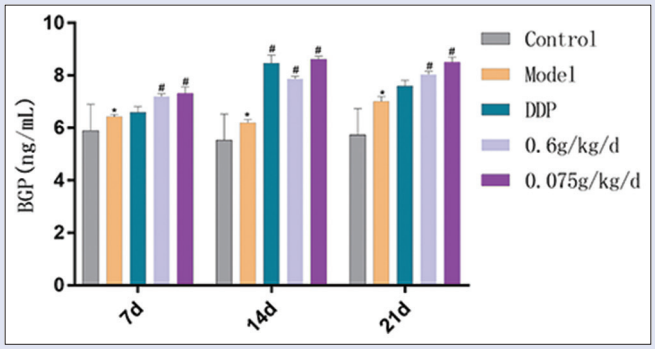

Figure 8: BGP changes of rats in different experimental groups ($\bar{X}$ ± SD, n = 8) (Compared with the blank group, $P < 0.01$ is **, $P < 0.05$*; compared with the model group, $P < 0.01$ is $^{\#\#}$, $P < 0.05$ is $^{\#}$)

in three stages.[25] The first stage is the formation of a hematoma. The occurrence of fracture is accompanied by the destruction of blood vessels. Exposure of platelets outside the blood vessels leads to the formation of hematomas. In the second stage, during the formation of the blood callus, the inner and outer membranes of the bone ossify to form the callus, which provides an initial structural scaffold for bone formation.[26] Macrophages in the fracture space guide mesenchymal stem cells to differentiate into cartilage, and bone marrow mesenchymal stem cells grow into osteocyte differentiation. In the third stage, the bone healing period, the blood flow at the fracture site increases toward the cartilaginous callus through a large number of blood vessels. In the fourth stage, the plastic phase, the balance between osteoblasts and osteoclasts initiates bone remodeling, slowly recovering the normal shape of the bone, and finally healing the fracture site.

AKP is mostly derived from bone secretion, and part of them was synthesized by bones, spleen, liver, kidneys and other organs. Osteoblasts produce a large number of inorganic phosphate ions while synthesizing AKP.[27] The synthesis of calcium phosphate in bone tissue is completed by the combination of phosphate and calcium ions. The level of AKP in the serum can reflect the activity of osteoblasts, and AKP is often used as a marker to indicate the activity of osteoblasts. This experimental study found that after 14 days of the administration, the serum AKP levels of rats in the positive drug group and the CS polysaccharide high- and low-dose groups were significantly higher than those in the model group. CS polysaccharides can promote the healing of fractures by increasing the activity of osteoblasts and the secretion of AKP.

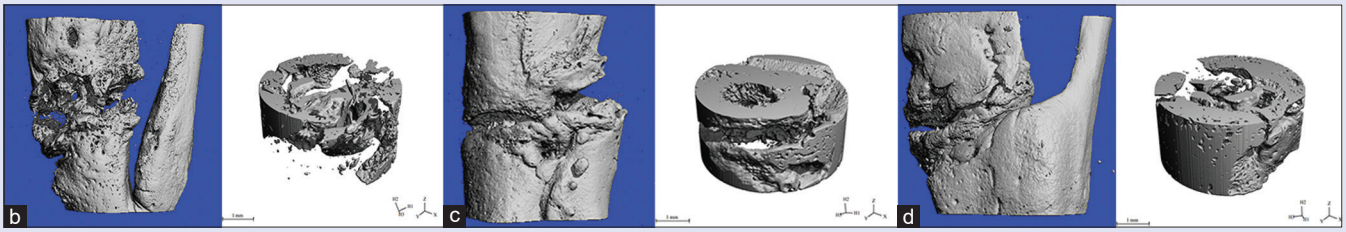

Figure 9: Micro-CT scanning analysis of tibial fracture callus in each group of rats (b); model group; (c) positice drug group; (d) the CS polysaccharide high-dose group

Table 1: Comparison of micro-CT detection parameters of each group ($\bar{X}$±SD, n=3) (Compared with the model group, $P<0.01$ is##, $P<0.05$ is#)

Group	TV (mm³)	BV （mm³）	BV/TV
Model	49.8779±5.12	10.2574±6.14	0.2056±3.22
DDP	49.8779±3.22	22.7851±7.15	0.4568±5.32#
0.6 g/kg/d	49.8779±6.13	23.8292±1.27	0.4778±6.17#

ACP is derived from bones, blood cells, prostate, and other organs. It is often distributed in the phagocytic area of osteoclasts and the space between osteoclasts and bone. It plays an indispensable role in bone resorption activities.[28] During the fracture healing period, osteoclasts play a role mainly by absorbing necrotic bone, removing residues, and participating in bone reconstruction. This experimental study found that the serum ACP level of SD rats in the high and medium doses of CSPs increased significantly after 14 days of administration, and was also at a higher level after 21 days of the administration, which indicated that CS polysaccharides can enhance osteoclasts activity and promote the absorption of local necrotic bone and promote bone reconstruction.

BGP is a specific protein synthesized and secreted by osteoblasts, which can reflect the activity of osteoblasts and participate in calcium regulation in the body. In the process of bone formation, it promotes matrix calcification and accelerates the maturation of the bone matrix.[29] This experimental study found that after 21 days of administration, the serum BGP level of SD rats in the CS polysaccharides group increased significantly, indicating that CS polysaccharides can promote the maturation and calcification of bone matrix after fracture.

DISCUSSION

This experimental study found that after seven days of administration, the serum AKP level of rats in the positive control group and the high and low doses of CSPs was higher than that of the model group, and did not reach a very significant level. After 14 days of the administration, the positive control group and the serum AKP level of rats in the CSPs high- and low-dose groups were significantly higher than that of the model group. Comparing the serum AKP levels on 7 days and 14 days combined with X-ray images, it shows that 7 days is the period when the fracture just starts to heal. The liver began to secrete AKP, but did not reach the maximum level. It reached the maximum level at 14 days. The results of micro-CT showed that the polysaccharide high-dose group and the positive drug group had more callus at the fracture end and the fracture line was close to healing. Through rat serum indicators AKP, ACP, and BGP combined with pathological slices and micro-CT imaging, the results show that CSPs have a good repair effect on SD rats tibia fractures, significantly shortens the fracture healing time, and promotes SD rats tibia fractures heal.

CONCLUSION

In summary, combined with histopathological observations, X-ray imaging results analysis, micro-CT analysis and serum index analysis, it can be seen that CSPs promote the synthesis of osteoblasts, secrete AKP, BGP, and osteoclasts secrete ACP, thereby increasing the growth rate. After 14 days of administration, the serum AKP levels of the rats in the high-dose CS polysaccharide group and the positive drug group were significantly higher than those in the model group. The results showed that CS polysaccharide promoted fracture healing by increasing the AKP secretory activity of osteoblasts. After 21 days of the administration, the serum ACP secretion of the rats in the high- and medium-dose groups of CS polysaccharide was significantly increased, and bone reconstruction was achieved by increasing the activity of osteoclasts and promoting the absorption of local necrotic bone. BGP represents the activity of osteoblasts, and the level of BGP in the CS polysaccharide group increased significantly after 21 days of the administration, indicating that CS polysaccharide can promote fracture healing by promoting the maturation and calcification of the bone matrix. The number of bone cells can effectively promote the healing of tibia fractures in SD rats. CS polysaccharide has a significant improvement effect on fracture-related biochemical indicators of SD rats and promotes the maturation and calcification of the matrix in the late stage of fracture, which can accelerate the rate of collagen synthesis and calcium salt precipitation and improve the quality of the callus, thus promotes the healing of fractures. The mechanism of CS polysaccharides in promoting tibial fracture healing in SD rats needs further study.

Authors statements

Zhihong Zhang: Writing-original draft, Writing-review and editing. Yuanning Zeng: Data calculation and Validation. Donghui Peng: Validation. Na Xing: Review. Haodong Bai: Review. Yuxin Li: Investigation. Na Cui: Investigation. Huilin Su: Investigation. Tingting Qiao: Investigation. Congjing Shi: Investigation. Haixue Kuang: Conceptualization, Methodology, Resources. Qiuhong Wang: Writing-review and editing, Conceptualization, Methodology, Resources.

Financial support and sponsorship

This work was financially supported in part by National Key R&D Program Project (2018YFC1707100), and National Natural Science Foundation of China (8177141630), and Guangdong Province Key Field R&D Program Project (2020B1111120002).

Conflicts of interest

There are no conflicts of interest.

REFERENCES

1. Cheng J, Li Y, Zang T, Liu F, Jin X, Ren Q, Liu B. MiR-21 accelerates tibial fracture healing in rats by regulating TGF-β1/smad signaling pathway. Panminerva Med. 2020. doi: 10.23736/S0031-0808.19.03799-6. Epub ahead of print. PMID: 31985186.
2. Wang X, Su N. Neurokinin-1-tachykinin receptor agonist promotes diabetic fracture healing in rats with type 1 diabetes via modulation of Wnt/β-catenin signalling axis. Saudi J Biol Sci 2021;28:2139-45.
3. Menger MM, Bremer P, Scheuer C, Rollmann MF, Braun BJ, Herath SC, *et al.* Pantoprazole

impairs fracture healing in aged mice. Sci Rep 2020;10:22376.

4. Wong RW, Rabie AB. Traditional Chinese medicines and bone formation–A review. J Oral Maxillofac Surg 2006;64:828-37.
5. Wahid S, Alqahtani A, Alam Khan RA. Analgesic and anti-inflammatory effects and safety profile of Cucurbita maxima and Cucumis sativus seeds. Saudi J Biol Sci 2021;28:4334-41.
6. Mallek-Ayadi S, Bahloul N, Kechaou N. Phytochemical profile, nutraceutical potential and functional properties of Cucumis melo L. seeds. J Sci Food Agric 2019;99:1294-301.
7. Mukherjee PK, Nema NK, Maity N, Sarkar BK. Phytochemical and therapeutic potential of cucumber. Fitoterapia 2013;84:227-36.
8. Sotiroudis G, Melliou E, Sotiroudis TG, Chinou I. Chemical analysis, antioxidant and antimicrobial activity of three Greek cucumber (Cucumis sativus) cultivars. J Food Biochem 2010;34:61-78.
9. Cheng H, Huang G. Extraction, characterisation and antioxidant activity of Allium sativum polysaccharide. Int J Biol Macromol 2018;114:415-9.
10. Shang XL, Liu CY, Dong HY, Peng HH, Zhu ZY. Extraction, purification, structural characterization, and antioxidant activity of polysaccharides from Wheat Bran. J Molecular Structure. 2021. doi:10.1016/j.molstruc.2021.130096.
11. Wu J, Li C, Bai L, Wu J, Bo R, Ye M, *et al.* Structural differences of polysaccharides from Astragalus before and after honey processing and their effects on colitis mice. Int J Biol Macromol 2021;182:815-24.
12. Yu Y, Shen M, Song Q, Xie J. Biological activities and pharmaceutical applications of polysaccharide from natural resources: A review. Carbohydr Polym 2018;183:91-101.
13. Chen X, Li T, Qing D, Chen J, Zhang Q, Yan C. Structural characterization and osteogenic bioactivities of a novel Humulus lupulus polysaccharide. Food Funct 2020;11:1165-75.
14. Nai J, Zhang C, Shao H, Li B, Li H, Gao L, *et al.* Extraction, structure, pharmacological activities and drug carrier applications of Angelica sinensis polysaccharide. Int J Biol Macromol 2021;183:2337-53.
15. Wang N, Wang X, Huang X, Mao Z, Zhang Y, Yu Y, *et al.* Monosaccharide composition analysis of immunomodulatory polysaccharides by on-line hollow fiber microextraction with high-performance liquid chromatography. J Sep Sci 2016;39:818-26.
16. Wang XY, Zhang DD, Yin JY, Nie SP, Xie MY. Recent developments in Hericium erinaceus polysaccharides: Extraction, purification, structural characteristics and biological activities. Crit Rev Food Sci Nutr 2019;59(sup1):S96-115.
17. Zhang ZP, Shen CC, Gao FL, Wei H, Ren DF, Lu J. Isolation, purification and structural characterization of two novel water-soluble polysaccharides from Anredera cordifolia. Molecules 2017;22:1276.
18. Shang J, Ma B, Zhu G, Dong P, Wang C, Gu X, *et al.* Role of Zip1 in the regulation of NPY expression by MLT to promote fracture healing in rats. Eur J Histochem 2020;64(s2):3183.
19. Yang G, Duan X, Lin D, Li T, Luo D, Wang L, *et al.* Erratum: Rapamycin-induced autophagy activity promotes bone fracture healing in rats. Exp Ther Med 2021;21:318.
20. Li YF, Luo E, Feng G, Zhu SS, Li JH, Hu J. Systemic treatment with strontium ranelate promotes tibial fracture healing in ovariectomized rats. Osteoporos Int 2010;21:1889-97.
21. Shefelbine SJ, Simon U, Claes L, Gold A, Gabet Y, Bab I, *et al.* Prediction of fracture callus mechanical properties using micro-CT images and voxel-based finite element analysis. Bone 2005;36:480-8.
22. Shi HF, Cheung WH, Qin L, Leung AH, Leung KS. Low-magnitude high-frequency vibration treatment augments fracture healing in ovariectomy-induced osteoporotic bone. Bone 2010;46:1299-305.
23. Gu Y, Zhou J, Wang Q, Fan W, Yin G. Ginsenoside Rg1 promotes osteogenic differentiation of rBMSCs and healing of rat tibial fractures through regulation of GR-dependent BMP-2/SMAD signaling. Sci Rep 2016;6:25282.
24. Shi L, Liu Y, Yang Z, Wu T, Lo HT, Xu J, *et al.* Vasoactive intestinal peptide promotes fracture healing in sympathectomized mice. Calcif Tissue Int 2021;109:55-65.
25. Nakajima A, Shimoji N, Shiomi K, Shimizu S, Moriya H, Einhorn TA, *et al.* Mechanisms for the enhancement of fracture healing in rats treated with intermittent low-dose human parathyroid hormone (1-34). J Bone Miner Res 2002;17:2038-47.
26. Ozaki A, Tsunoda M, Kinoshita S, Saura R. Role of fracture hematoma and periosteum during fracture healing in rats: interaction of fracture hematoma and the periosteum in the initial step of the healing process. J Orthop Sci 2000;5:64-70.
27. Zhao XG, Zhao GF, Chen YJ, Ma YF, Jiang GY. A study on the mechanism of traumatic brain injury affecting the speed of bone fracture healing. Chin J Emerg Med 2007;16:936-9.
28. Li J, Cheah K, Zhou Z. Bone fracture healing in Laminopathy-based premature aging; 2006.
29. Sarisözen B, Durak K, Dinçer G, Bilgen OF. The effects of vitamins E and C on fracture healing in rats. J Int Med Res 2002;30:309-13.